

Structural distortion and electronic properties of NiO under high pressure: an *ab initio* GGA+*U* study

This article has been downloaded from IOPscience. Please scroll down to see the full text article.

2006 J. Phys.: Condens. Matter 18 9691

(<http://iopscience.iop.org/0953-8984/18/42/015>)

View [the table of contents for this issue](#), or go to the [journal homepage](#) for more

Download details:

IP Address: 129.252.86.83

The article was downloaded on 28/05/2010 at 14:25

Please note that [terms and conditions apply](#).

Structural distortion and electronic properties of NiO under high pressure: an *ab initio* GGA + *U* study

Wei-Bing Zhang¹, Yu-Lin Hu¹, Ke-Li Han² and Bi-Yu Tang¹

¹ Department of Physics, Xiangtan University, Hunan Province, 411105, People's Republic of China

² Center for Computational Chemistry and State Laboratory of Molecular Reaction Dynamics, Dalian Institute of Chemical Physics, Chinese Academy of Sciences, Dalian 116023, People's Republic of China

E-mail: Tangbiyu@xtu.edu.cn

Received 15 June 2006, in final form 20 August 2006

Published 6 October 2006

Online at stacks.iop.org/JPhysCM/18/9691

Abstract

The structural distortion and electronic properties of NiO under high pressure are investigated by means of first-principles calculations within the density functional theory (DFT) in the generalized gradient approximation (GGA). The strong electronic correlations are also taken into account in the form of GGA + *U*. Recent experiments implied that previous local density approximation (LDA) calculations incorrectly predicted structural distortion under high pressure, especially above 60 GPa. The present results show that even GGA calculations do not give a proper description of structural distortion under high pressure, although much improved structural and bulk properties are obtained. When strong correlations are included, overall agreement of the structural distortions of NiO under high pressure is obtained. The lattice constants *a* and *c* as well as the axial ratio *c/a* are in good agreement with experiment over the entire experimental pressure range. The successful prediction of the structural distortion of GGA + *U* can be attributed to the reasonable description of nearest-neighbour magnetic exchange interactions. In addition, we also analyse the density of states under different pressures. Present results indicate that, with increasing pressure, the bandwidth increases and the bandgap transits from being a mixture of charge-transfer and Mott–Hubbard type towards solely Mott–Hubbard type.

1. Introduction

The behaviour of 3d transition-metal monoxides (TMMO) such as NiO under high pressure plays an extremely important role in condensed matter physics and geophysics. Because they exhibit a rich variety of electronic and magnetic phenomenon [1, 2], 3d TMMO have attracted a lot of attention over the past decades. However, as a prototype of a Mott insulator, some

properties of NiO such as structural distortion under high pressure are far from being fully understood.

NiO is known to be an fcc type-II antiferromagnetic insulator with Néel temperature T_N of 523 K. It crystallizes in the simple cubic rocksalt ($B1$) structure above T_N but becomes a rhombohedrally distorted $B1$ ($rB1$) structure compressed along the [111] direction with rhombohedral angle α_{rh} equal to 60.08° [3] when the temperature is below T_N . Although the electronic structure and magnetic properties of NiO at ambient pressure have been studied extensively [4–20], there are only a few works concerning the structural distortion of NiO under high pressure. Experimentally, for geophysical interests, the equation of state (EOS) has been measured by static compression [21] up to 28 GPa and by shock compression [22] up to 147 GPa. No pressure-induced structural phase transition was observed in the experimental pressure range [21–24]. Recently, Eto *et al* [3] investigated the pressure effect of the structural distortion up to 141 GPa by static compression with two different pieces of equipment (named A and B), they found that the compression along the [111] direction increased with pressure. The lattice parameters a and c expressed in the hexagonal lattice as well as the axial ratio c/a monotonically decreased with pressure, and the pressure coefficient of c/a was almost constant over the experimental pressure region. However, early local spin density function calculations [24] suggested that the pressure coefficient of c/a became large significantly above 60 GPa, which was markedly different from the experimental result.

From a theoretical point of view, because NiO is a classical example of strongly correlated systems and the structural distortion is very slight, it is difficult to obtain accurate structural properties under high pressure. Using the local spin density approximation (LDA), Sasaki [24] investigated the structural change of NiO with pressure. As mentioned previously, the calculation suggested that lattice distortion increased with pressure and the pressure coefficient of c/a became significantly large above 60 GPa, but the latter was not observed in recent experiments [3]. The conflict between theory and experiment indicates that the LDA is inadequate to describe the structural properties of NiO even at high pressure. Although the electronic correlation will become weak because of increasing screening, it has been proved that correlation effects still play a very important role under high pressure both experimentally [25] and theoretically [26, 27]. To our knowledge, no calculations including strong electronic correlations have so far been carried out to investigate the structural distortion of NiO under high pressure.

In order to shed light on the experimental results and to get a better understanding of the structural distortion in TMMO under high pressure, we present here the structural properties and related electronic structure as a function of pressure within generalized gradient approximations (GGA); the strong on-site Coulomb repulsion between Ni 3d electrons are also included in the form of $GGA + U$. Although there are many theories such as Hartree–Fock (HF) [11], GW approximation [12, 13], self-interaction corrections (SIC) [14, 15], hybrid density functional like B3LYP [16] and DFT + U [17–20] which have been developed to overcome the limitations of ordinary density functional theory, it is well documented that $GGA + U$ has been successfully applied to strongly correlated systems, which could predict accurate structural and magnetic properties [28–31] and is also applied to the optimization of atomic geometries under pressure [29, 32]. Recent work has demonstrated that $GGA + U$ could lead to significant advances in the description of molecular adsorption (CO, NO) on NiO(100) surfaces [20, 33].

This paper is organized as follows. The computational method is given in section 2. The structural properties and electronic structure are presented and discussed in sections 3. The conclusion can be found in section 4.

2. Computational methods

All calculations have been performed with the Vienna *ab initio* Simulation Package (VASP) [34–38], a first-principles plane-wave code based on spin-polarized density functional theory. In order to investigate structural distortion under high pressure, it is crucial to get an accurate lattice constant. It is known that LDA calculation tends to predict too small a lattice constant, so in this paper generalized gradient corrections added in the form of the Perdew–Wang functional [39] were chosen for the exchange correlation functional, the spin interpolation of Vosko *et al* [40] was also used. The interaction between ions and valence electrons was described by the projector augmented-wave (PAW) method [41]. The Kohn–Sham equations were solved via iterative matrix diagonalization based on the minimization of the norm of the residual vector to each eigenstate and optimized charge- and spin-mixing routines [42–44].

To take into account the electronic correlation, a simple rotationally invariant DFT + U version proposed by Dudarev *et al* [17, 19, 45] was used. In this method, parameters U and J represented on-site Coulomb interaction energy and exchange energy, respectively. The parameters U and J were not used separately, only their difference $U - J$ was meaningful. In the present calculations J was kept fixed at 1 eV. A detailed description of the DFT + U method can be found in [20, 46]. Resonant inelastic x-ray scattering (RIXS) [25] experiments suggested that the Coulomb interaction between the 3d electrons of NiO did not change appreciably with pressure up to 100 GPa although it is expected that the electronic correlation would become weak since screening increased with pressure. So the change of U with pressure has been neglected in this paper, as have many authors in other systems such as LaMnO₃ [32]. Using GGA + U with $U - J = 5.3$ eV, Rohrbach *et al* [20] obtained an improved description of a wide range of bulk properties of NiO. We also checked the bulk properties with $U - J$ and found that a value of $U - J = 5.3$ eV led to both an improved description of the bulk properties and lattice distortion at ambient pressure. So $U - J = 5.3$ eV was used in our calculations, $U - J = 7$ eV suggested by constrained LDA computations [19] and a smaller value $U - J = 2$ eV were also computed for comparison.

All results reported in this paper were carried out on a rhombohedral antiferromagnetic supercell including two NiO formula unit cells. Convergence tests have been checked carefully both for plane-wave cutoff energy and k point sampling. A plane-wave basis set expanded in energy showed a cutoff of 600 eV and k points sampling with a mesh of points $8 \times 8 \times 8$ generated by the scheme of Monkhorst–Pack [46] ensured a convergence accuracy with total energy difference less than 3 meV/atom. The optimizations of unit cell shape for each volume were performed using the conjugate gradient method and a Gaussian-smearing with a width of 0.2 eV. Forces acting on atoms and stress tensors on unit cells were used in the optimization process. For total energy and DOS calculations, the integration over the Brillouin zone was performed using the linear tetrahedron method with Blöchl corrections [47–49]. The calculated total energies as a function of volume were fitted to the Murnaghan equation of state (EOS) [50] to obtain equilibrium volume V_0 , bulk modulus B_0 and its pressure derivatives B'_0 .

3. Results and discussion

3.1. Properties at ambient pressure

The results of ground-state properties including equilibrium volume V_0 , bulk modulus B_0 and pressure derivative B'_0 after full relaxation of the cell shape are listed in table 1. From the table, it is very clearly seen that GGA and GGA + U both give quite reasonable results. First

Table 1. The calculated equilibrium volumes (V_0), bulk modulus B_0 and pressure derivative of the bulk modulus B'_0 using GGA and GGA + U . The experimental value and earlier LDA calculation results are also listed.

	V_0 (\AA^3)	B_0 (GPa)	B'_0	Pressure range (GPa)
GGA	36.72	197	5.71	0–9.3
		200	4.21	0–62.2
		206	3.91	0–140.0
GGA + U ($U - J = 5.3$ eV)	36.81	184	4.93	0–9.04
		189	3.91	0–64.2
		193	3.67	0–147.3
LDA ^a	35.22	236	4.28	0–60
Eto <i>et al</i> ^b	36.44	192(4)	4.0	0–9.3
		203(2)	4.0	0–60.1
		210(2)	4.0	0–141.7
Huang ^c		187	4.0	0–6.6
Noguchi <i>et al</i> ^d		191	3.9	0–147.6

^a Reference [24].

^b Reference [3].

^c Reference [21].

^d Reference [22].

we draw your attention to the equilibrium volume, which is very important to the equation of state, because an improper equilibrium volume will lead to a large discrepancy of the pressure–volume curve at low pressure. The obtained equilibrium volumes using GGA and GGA + U ($U - J = 5.3$ eV) are 36.72 and 36.81 \AA^3 respectively. Compared with an LDA result of 35.22 \AA^3 [24], both results are closer to the experimental volume of 36.44 \AA^3 [3].

It is well known that B_0 is sensitive to the pressure (volume) range which is used in the fitting procedure. In order to compare with previous calculations, we first determine the bulk modulus from the pressure range of 0–60 GPa, which was also used in the earlier LDA calculations [24]. The bulk modulus obtained with GGA and GGA + U is 200 and 189 GPa respectively which are very close to the experimental value [3] of 203(2) GPa in a similar pressure (volume) range, whereas previous LDA calculations gave a result of 236 GPa. The bulk modulus in other pressure (volume) ranges were also calculated and compared with experiment directly. The bulk moduli obtained using both methods in three pressure ranges are a little lower than Eto's experiments, but agree well with other experimental data [21, 22].

Figure 1 gives the volume of a hexagonal unit cell as a function of pressure obtained using GGA and GGA + U , together with different experimental data [3, 21, 22]. Both results are in good agreement with experiments, although a very small difference on the pressure–volume curve appears under high pressure, while previous LDA calculations [24] give a large discrepancy at low pressure. This results from the fact that the LDA predicts a too small equilibrium volume, as mentioned above. Pressure–volume curves with cubic $B1$ structure were also calculated. Our results indicate that as lattice distortion becomes large with pressure, a large difference of the pressure–volume relationship between cubic $B1$ and $rB1$ structure will appear under high pressure.

Although GGA gives a much improved bulk property, it is well known that GGA gives too small a bandgap and magnetic moment. Present GGA calculations predict the bandgap and magnetic moment to be about 0.5 eV and 1.28 μ_B whereas the GGA + U with $U - J = 5.3$ eV can give a much larger bandgap and magnetic moment. The values are 3.0 eV and 1.69 μ_B

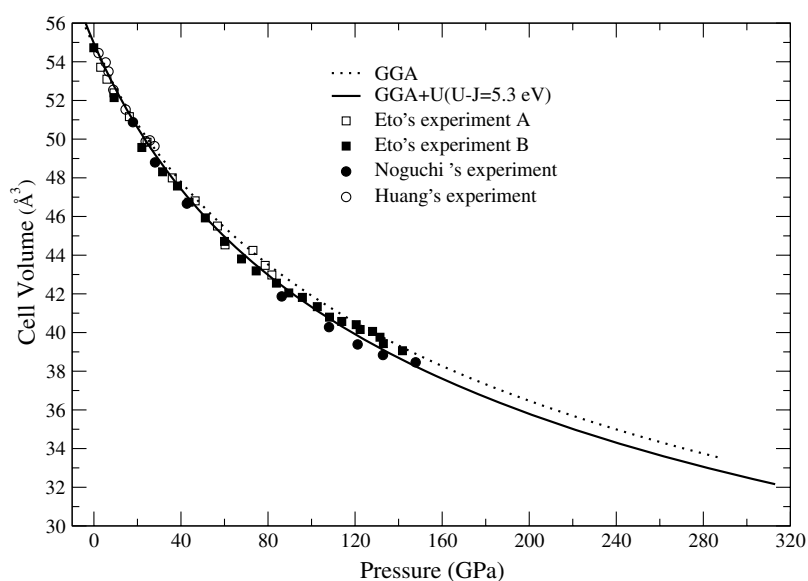


Figure 1. Pressure dependence of a hexagonal unit cell volume of NiO (three formula unit cells) calculated using GGA + U and GGA, together with experimental data taken from [3] and [21, 22].

which are similar to other DFT + U calculations in the literature [17–20]. The structural distortions under ambient pressure with different U are also examined. All calculations predict the ground state to have AFII ordering and the cell slightly compressed along the [111] direction (except for $U \geq 8$ eV). With increasing U , the axial ratio first increases fast then shows a weak dependence on U with further increasing U . The axial ratio obtained with GGA is 2.4288 (rhombohedral angle is 60.38°), underestimating the experimental axial ratio 2.4457(1) [3, 51] (angle is $60.07(8)^\circ$) at zero temperature. In other words, GGA overestimates the structural distortion. The overestimation of the rhombohedral distortion in GGA calculation was also found in other 3d transition-metal monoxides such as MnO [52]. However, compared with an LDA value of 2.42, the present GGA result is also closer to the experimental value. The calculated axial ratio with $U - J = 5.3$ eV is 2.4493 (rhombohedral angle is about 60.01°), which is in agreement with experiment. Moreover GGA + U with $U - J = 5.3$ eV also gives a reasonable description for the structural distortion of NiO under high pressure as shown below.

In order to check the possible structural phase transition from $B1$ ($rB1$) to $B2$ structure, which has been observed in most of the monoxides with $B1$ structure, we calculate the total energies of NiO with $B2$ structure using GGA at different volumes. The obtained phase transition pressure from the $rB1$ structure to the $B2$ structure is about 450 GPa, which is much larger than the 318 GPa obtained using the LDA [24]. Both values are also much larger than the considered pressure. It indicates that there is no pressure-induced structural phase transition appearing in the present pressure range, so all results reported in this paper are performed on $B1$ ($rB1$) structure.

3.2. Structural distortion under high pressure

Now let us focus on the result of structural distortion under high pressure. Pressure dependence of the lattice parameters a , c and c/a calculated with GGA and GGA + U are given in figure 2. For comparison, experimental data from [3] and LDA results from [24] are also

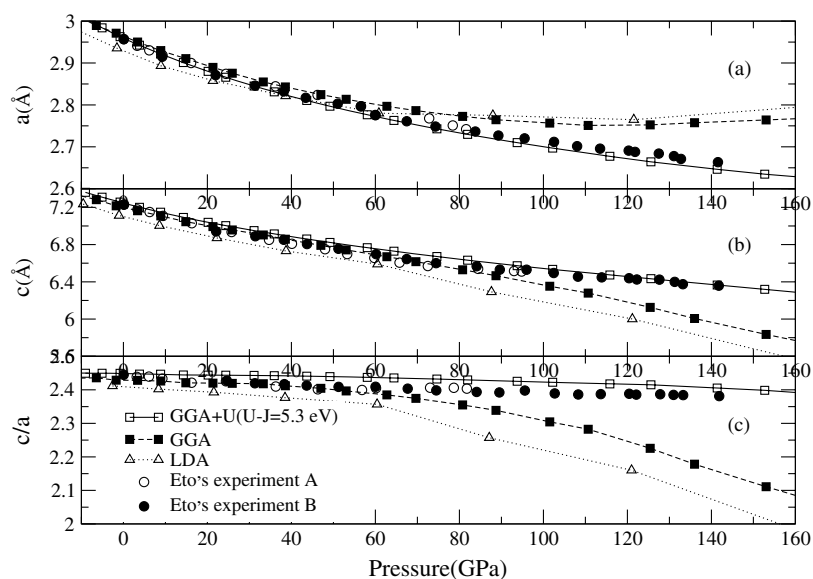


Figure 2. Pressure dependence of structural parameter a (upper panel), c (middle) and c/a (lower panel) of the distorted $B1$ structure for GGA and GGA + U ($U - J = 5.3$ eV), together with LDA calculation results from [24] and experimental data taken from [3].

included. The GGA results are very similar to previous LDA results [24], lattice parameter a exhibits nonmonotonic behaviour under pressure: it decreases below about 120 GPa and increases above 120 GPa. Also, c/a changes significantly above 60 GPa. However, it is very clearly seen that the results of a , c and c/a obtained with GGA are closer to the experiment, especially at low pressure, than with the LDA. But in Eto's experiment [3], both a and c decrease monotonically with increasing pressure, and the pressure coefficient of c/a is almost constant over the experimental pressure. Moreover, figure 2 also shows that both GGA and LDA predict too small an axial ratio c/a especially above 60 GPa, and this deviation from experiment becomes larger with pressure. Although it is expected that electronic correlation may become weaker with pressure since screening increases [26], the discrepancy between theories and experiment even above 60 GPa shows that the strong electronic correlations still play a very important role in the experimental pressure range.

As shown above, both GGA and LDA show discrepancies with the experimental results. All these discrepancies can be removed with inclusion of the strong electronic correlations. From figure 2, it can be seen that the GGA + U calculation with $U - J = 5.3$ eV can give an improved description for all lattice parameters of NiO in the experimental pressure range. In this range, both a and c decrease monotonically with pressure without an increase at high pressure, as predicted by ordinary DFT calculation. The axial ratio c/a decreases with pressure and the pressure derivative of c/a is almost constant over the entire pressure region, which are in agreement with experiment. For comparison, the structural distortions under high pressure with different $U - J$ are also investigated. As shown in figure 3, the axial ratio decreases with pressure for different $U - J$. It should be noticed that the value of c/a increases with the value of $U - J$. Present calculations also suggest that the transition pressure becomes higher with increasing $U - J$ and the value will be above 140 GPa only in the calculations with $U - J \geq 4$ eV. Experimentally, there is no sudden increase of pressure derivative of c/a in the entire pressure range. Therefore, only the calculations with $U - J \geq 4$ eV can give a proper

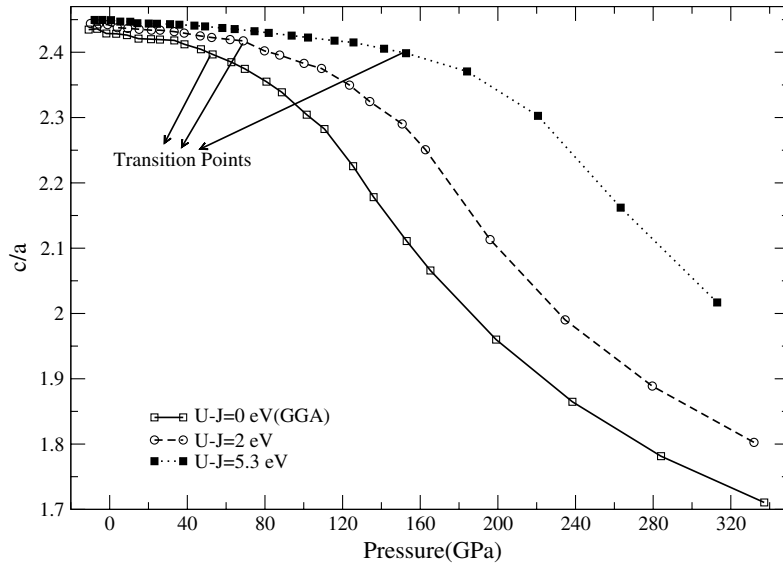


Figure 3. Pressure dependence of the axial ratio c/a for GGA + U with $U - J = 0$ eV (GGA), 2 eV and 5.3 eV. The result obtained with $U - J = 7$ eV is not shown in the figure. J is fixed at 1 eV.

description for the behaviour of NiO under high pressure. However, when the value of $U - J$ increases to 7 eV, the calculated axial ratio c/a is much smaller than the experimental value in the considered pressure, which implies that the strong electronic correlations are overestimated. Finally, we found that $U - J = 5.3$ eV, used in the present calculations, would be more appropriate.

To explain the calculation results, in Sasaki's work [24], the rhombohedral distortion was analysed by expanding the total energy with respect to the shear strain up to the fourth-order term and determining the coefficient of each term.

$$E(\varepsilon; V) \approx E_0(V) + a(V)\varepsilon + b(V)\varepsilon^2 + c(V)\varepsilon^3 + d(V)\varepsilon^4 + \dots \quad (1)$$

The higher-order terms can be neglected in this equation. Where $a(V)$ represents the magnetic distortion and $b(V)$ represents the elastic term, which functions as the restoring force when it has a positive value. $b(V)$ can be divided into two parts: electrostatic energy b_{es} with negative value and the band structure energy b_{bs} with positive value.

$$b(V) = b_{es} + b_{bs}(b_{es} \langle 0, b_{bs} \rangle 0). \quad (2)$$

The rhombohedral distortion under pressure is mainly governed by the second-order term $b(V)$ of ε . In general, $b(V)$ decreases with pressure, the change of the sign of $b(V)$ will result in an increase of the pressure coefficient of c/a . Because the ordinary DFT calculations fail in describing the 3d electronic correlation of NiO, Eto [3] suggested that both LDA and GGA may underestimate the band structural energy b_{bs} over the entire pressure range. This underestimation will lead to a decrease of $b(V)$, i.e. the restoring forces are underestimated, which results in a much larger lattice distortion than in the experiment.

On the other hand, the mechanism of rhombohedral distortion of MnO at ambient pressure has been discussed by Pask *et al* [52]. It is argued that the weak NN (nearest-neighbour) interaction plays the decisive role in the structural distortion, while the stronger NNN (next-nearest-neighbour) coupling through oxygen has nothing to do with it. Since NiO has similar

magnetic ordering and structure to MnO, it is expected that the conclusion could be applied to the case of NiO. So, the structural distortion of NiO should be driven by the NN exchange interaction. It is noted that direct magnetic interactions calculated using LDA by Oguchi *et al* [53] and by Moreira *et al* [54] are 5.3 and 11.9 meV respectively, which are much larger than the experimental value of 1.37 meV [55]. The overestimation of magnetic interactions also occurs in the case of MnO [52]. In order to clarify the underlying mechanism, we have calculated the magnetic interactions using GGA and GGA + U based on the Heisenberg spin Hamiltonian. The calculated NN magnetic interaction J_1 at ambient pressure using GGA is 2.41 meV, which still overestimates the experiment, while GGA + U gives a value of 1.73 meV, which is in good agreement with the experimental result. Moreover, we also examine the pressure effect of J_1 using GGA + U . The results indicate that the NN exchange interaction linearly increases with pressure and the pressure coefficient is basically constant. This is consistent with the structural distortion calculated using GGA + U . As shown above, the structural distortion calculated using GGA + U increases with pressure and the pressure coefficient of c/a is almost constant over the experimental pressure without the sudden increase found in ordinary DFT calculations. It seems that the overestimated J_1 in the case of LDA and GGA may provide too large driving forces, which will lead to the overestimated structural distortion of TMMO in ordinary DFT calculations.

3.3. Electronic structure

The discrepancy between the experiment and ordinary DFT calculations mainly results from the fact that ordinary DFT calculations have difficulty in describing the 3d electronic correlation. To understand the role of strong electronic correlation of NiO in electronic structure under high pressure, we report the density of states (DOS) of NiO at three different pressures on distorted $B1$ structure using GGA + U ($U - J = 5.3$ eV) after cell shape relaxation, together with GGA calculation for comparison. Electronic structural analyses are also performed on the cubic $B1$ structure (not shown in this paper). The results suggest the cell relaxations have a very slight effect on the electronic structure and the compressed lattice distortion even tends to enlarge bandgap.

As shown in figure 4, both in GGA and GGA + U , the shape of the electronic density of states does not change much with pressure while the density of states decrease and bandwidth increases monotonically. This is compatible with Shukla's experiment [25], in which the width of peaks increases and the position does not change appreciably. Other calculations using GGA [26] and B3LYP functional [27] also gave similar results. With increasing pressure, although bandwidth becomes large, the bandgap has a slight change in considered pressure range. The increasing bandwidths may reduce the bandgap. On the other hand, both the increased crystal-field splitting because of the volume compression and slight distortion tends to enlarge the gap. Finally, the bandgap has a slight change through balance between the above effects [27]. Resonant inelastic x-ray scattering (RIXS) experiments [25] also found that charge-transfer and correlation energies did not change appreciably up to 100 GPa. Both calculations also show that no metal-insulator transition and magnetic collapse appears in the experimental pressure range, although the bandgap will decrease at high pressure. It can be expected that, because bandwidth increases, metal-insulator transition and magnetic collapse will appear at a higher pressure with the bandgap closing, but this is beyond the scope of the present study.

However, it is very clearly seen in figure 5 that GGA + U gives a wider bandgap than GGA; moreover, it should be noticed that in the case of GGA + U , O 2p is mixed with Ni 3d at the top of the valence band, hence the bandgap is a mixture of charge transfer and Mott-Hubbard d-d type. Recent experiments [10] also gives evidence that the bandgap is mixture of charge

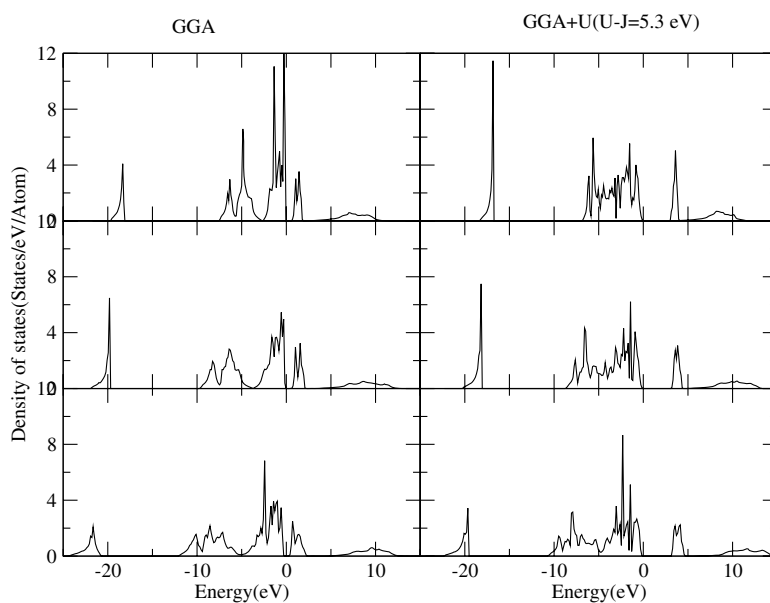


Figure 4. Calculated total DOS of NiO at selected pressures for GGA and GGA + U ($U - J = 5.3$ eV). Going from the top to bottom panel, the DOS refers to structures with increasing pressures equal to about 9, 60, 140 GPa. The energies are given relative to the top of the valence band.

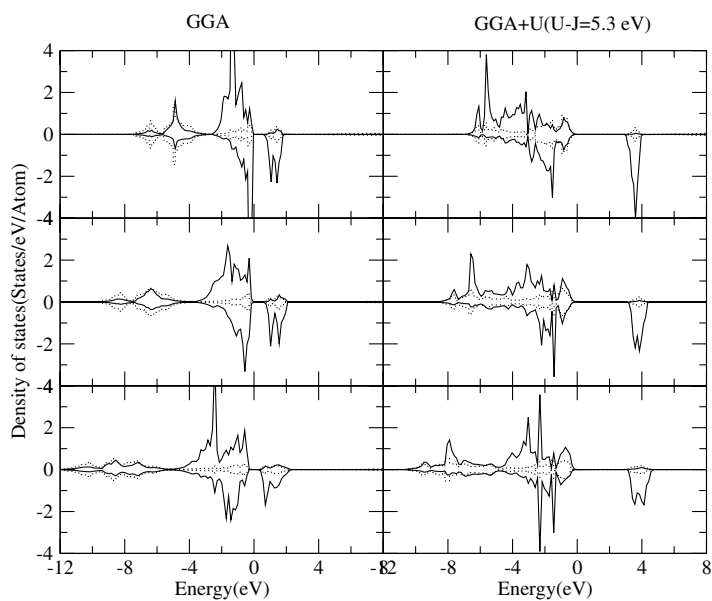


Figure 5. Orbital projected DOS (PDOS) of NiO at selected pressures for GGA and GGA + U ($U - J = 5.3$ eV). Going from the top to bottom panel, the DOS refers to structures with increasing pressures equal to about 9, 60, 140 GPa. The solid and dashed lines indicate Ni 3d and O 2p respectively. The energies are given relative to the top of the valence band.

transfer and Mott–Hubbard character. The bandgap calculated using GGA is pure character of Mott–Hubbard type with the top of valence bands dominated by Ni 3d. As increasing pressure,

the Ni 3d orbital enhances significantly over the O 2p, making the bandgap change from being a mixture of charge-transfer and Mott–Hubbard type towards pure Mott–Hubbard character.

As mentioned above, GGA + U gives much improved details of DOS in accord with experiment, while GGA calculations cannot correctly describe the details of electronic structure. The improper description of electronic structure may result in the discrepancies of structural distortion between GGA and experimental results.

4. Conclusions

In the present study, we have calculated structural distortion and electronic properties as a function of pressure using GGA and GGA + U . The calculation results suggest that although GGA gives much improved structure properties and bulk properties compared with LDA, the main discrepancy in structural distortion between experiment and theory still exists. The axial ratio c/a becomes extremely large at pressures above 60 GPa, which has not been observed in recent experiments. This discrepancy is because of the improper description of the electronic correlation between 3d electrons in ordinary DFT calculation. When the strong electronic correlations were included in the form of GGA+ U , we obtained overall agreement of structural distortion over the entire pressure range.

A simple analysis for structural distortion is also given. From this analysis, we found that ordinary DFT overestimated the NN exchange interaction which was known to be related closely to structural distortion. This overestimation may lead to overestimated driving forces and result in a large deviation of the structural distortion from experiment results. We also performed analysis in detail for the DOS with different pressures. Consistent with experiment, GGA + U gave a reasonable description of electronic structure. The present results suggest that the bandwidth increases appreciably with pressure while the bandgap has a slight change, and metal–insulator transition and magnetic collapse do not appear in the considered pressure range. Moreover, with increased pressure, the bandgap transits from being a mixture of charge-transfer and Mott–Hubbard type towards just Mott–Hubbard character.

These results show that the strong electronic correlations between 3d electrons still play a very important role in structural and electronic properties under high pressure even above 100 GPa. The present work also attempts to treat strongly correlated system under high pressure using DFT + U .

Acknowledgments

We would like to thank E G Wang for very useful discussions and help. This work is supported by the Open Project Program of Key Laboratory of Advanced Materials and Rheological Properties, Ministry of Education, China (KF0504).

References

- [1] Yoo C S *et al* 2005 *Phys. Rev. Lett.* **94** 115502
- [2] Fang Z, Terakura K, Sawada H, Miyazaki T and Solovyev I 1998 *Phys. Rev. Lett.* **81** 1027
- [3] Eto T, Endo S, Imai M, Katayama Y and Kikegawa T 2000 *Phys. Rev. B* **61** 14984
- [4] Sawatzky G A and Allen J W 1984 *Phys. Rev. Lett.* **53** 2339
- [5] Fender B E F and Jacobson A I 1968 *J. Chem. Phys.* **48** 990
- [6] Cheetham A K and Hope D A O 1983 *Phys. Rev. B* **27** 6964
- [7] Fujimori A and Minami F 1984 *Phys. Rev. B* **30** 957
- [8] Hühfner S, Osterwalder J, Riesterer T and Hulliger F 1984 *Solid State Commun.* **52** 793

- [9] Tjernberg O, Söderholm S, Karlsson U O, Chiaia G, Qvarford M, Nylén H and Lindau I 1996 *Phys. Rev. B* **53** 10372
- [10] Schuler T M, Ederer D L, Itza-Ortiz S, Woods G T, Callcott T A and Woicik J C 2005 *Phys. Rev. B* **71** 115113
- [11] Towler M D, Allan N L, Harrison N M, Saunders V R, Mackrodt W C and Apra E 1994 *Phys. Rev. B* **50** 5041
- [12] Aryasetiawan F and Gunnarsson O 1995 *Phys. Rev. Lett.* **74** 3221
- [13] Massidda S, Continenza A, Posternak M and Baldereschi A 1997 *Phys. Rev. B* **55** 13494
- [14] Svane A and Gunnarsson O 1990 *Phys. Rev. Lett.* **65** 1148
- [15] Szotek Z, Temmerman W M and Winter H 1993 *Phys. Rev. B* **47** 4029
- [16] Becke A D 1993 *J. Chem. Phys.* **98** 5648
- [17] Anisimov V I, Zaanen J and Andersen O K 1991 *Phys. Rev. B* **44** 943
- [18] Liechtenstein A I, Anisimov V I and Zaanen J 1995 *Phys. Rev. B* **52** R5467
- [19] Dudarev S L, Botton G A, Savrasov S Y, Humphreys C J and Sutton A P 1998 *Phys. Rev. B* **57** 1505
- [20] Rohrbach A, Hafner J and Kresse G 2004 *Phys. Rev. B* **69** 075413
- [21] Huang E 1995 *High Pressure Res.* **13** 307
- [22] Noguchi Y, Uchino M, Hikosaka H, Atou T, Kusaba K, Fukuoka F, Mashimo T and Syono Y 1999 *J. Phys. Chem. Solids* **60** 509
- [23] Clendenen R L and Drickamer H G 1966 *J. Chem. Phys.* **44** 4223
- [24] Sasaki T 1996 *Phys. Rev. B* **54** R9581
- [25] Shukla A, Rueff J P, Badro J, Vanko G, Mattila A, de Groot F M F and Sette F 2003 *Phys. Rev. B* **67** R081101
- [26] Cohen R E, Mazin I I and Isaak D G 1997 *Science* **275** 654
- [27] Feng X B and Harrison N M 2004 *Phys. Rev. B* **69** 035114
- [28] Rohrbach A, Hafner J and Kresse G 2003 *J. Phys.: Condens. Matter* **15** 979
- [29] Rollmann G, Rohrbach A, Entel P and Hafner J 2004 *Phys. Rev. B* **69** 165107
- [30] Rohrbach A, Hafner J and Kresse G 2004 *Phys. Rev. B* **70** 125426
- [31] Lampis N, Franchini C, Satta G, Geddo-Lehmann A and Massidda S 2004 *Phys. Rev. B* **69** 064412
- [32] Trimarchi G and Binggeli N 2005 *Phys. Rev. B* **71** 035101
- [33] Rohrbach A and Hafner J 2005 *Phys. Rev. B* **71** 045405
- [34] Kresse G and Hafner J 1993 *Phys. Rev. B* **47** 558
- [35] Kresse G and Hafner J 1994 *Phys. Rev. B* **49** 14251
- [36] Kresse G and Furthmüller J 1996 *Phys. Rev. B* **54** 11169
- [37] Kresse G and Furthmüller J 1996 *Comput. Mater. Sci.* **6** 15
- [38] Kresse G and Joubert D 1999 *Phys. Rev. B* **59** 1758
- [39] Perdew J P, Chevary J A, Vosko S H, Jackson K A, Pederson M R, Singh D J and Fiolhais C 1992 *Phys. Rev. B* **46** 6671
- [40] Vosko S H, Wilk L and Nusair M 1980 *Can. J. Phys.* **58** 1200
- [41] Blöchl P E 1994 *Phys. Rev. B* **50** 17953
- [42] Wood D M and Zunger A 1985 *J. Phys. A: Math. Gen.* **18** 1343
- [43] Johnson D D 1988 *Phys. Rev. B* **38** 12807
- [44] Pulay P 1980 *Chem. Phys. Lett.* **73** 393
- [45] Bengone O, Alouani M, Blöchl P and Hugel J 2000 *Phys. Rev. B* **62** 16392
- [46] Monkhorst H J and Pack J D 1976 *Phys. Rev. B* **13** 5188
- [47] Jepsen O and Anderson O K 1971 *Solid State Commun.* **9** 1763
- [48] Methfessel M and Paxton A T 1989 *Phys. Rev. B* **40** 3616
- [49] Blöchl P E, Jepsen O and Andersen O K 1994 *Phys. Rev. B* **49** 16223
- [50] Murnaghan F D 1944 *Proc. Natl Acad. Sci. USA* **30** 244
- [51] Toussaint C J 1971 *J. Appl. Crystallogr.* **4** 293
- [52] Pask J E, Singh D J, Mazin I I, Hellberg C S and Kortus J 2001 *Phys. Rev. B* **64** 024403
- [53] Oguchi T, Terakura K and Williams A R 1983 *Phys. Rev. B* **28** 6443
- [54] Moreira I P R, Illas F and Martin R L 2002 *Phys. Rev. B* **65** 155102
- [55] Shanker R and Singh R A 1973 *Phys. Rev. B* **7** 5000